Effect of Molecular Architecture on Polymer–Surface Adsorption

ANNA C. BALAZS

Materials Science and Engineering Department, University of Pittsburgh, Pittsburgh, Pennsylvania 15261

Received August 20, 1992

Introduction

The behavior of polymers at interfaces makes them a crucial ingredient in a broad range of contemporary manufacturing needs, including the production of food, pesticides, high-performance materials, and the fuel to meet our energy requirements. In particular, polymer-modified surfaces facilitate every stage of oil and coal production. From drilling and mining to transporting and processing, and finally to cleaning up undesirable byproducts, polymer–surface interactions enhance the commercial viability of these processes.[1] For example, by adsorbing at the fuel–water interface, polymers stabilize oil–water emulsions and prevent flocculation of coal particles in solution.[2] This, in turn, allows the fuels to be processed and transported. Furthermore, polymer coatings prevent the corrosion of iron and steel that are used in oil and gas pipelines. In the case of spills, macromolecular surfactants are used to disperse oil slicks.

Another area of significant technological importance is the production of new, more energy-efficient materials. Composite materials in which polymers are bound to ceramic, metal, or other polymer substrates are seen as a key development in this area. Polymer–surface interactions also play a critical role in biomedical applications. In particular, coating surfaces with polymers can enhance the biocompatibility of artificial implants.[3]

In order to optimize the properties described above, it is important to isolate the factors that influence the interfacial activity of polymer chains. In this Account, we review theoretical models and computer simulations used to determine the effects of polymer architecture and surface morphology on the properties of chains at penetrable and impenetrable interfaces. As we demonstrate below, the interfacial tension between oil–water mixtures as well as the mechanical properties of polymer composites can be controlled by varying the arrangement of the different repeat units (the sequence distribution) in the copolymer additives. We also find that the structure of polymer coatings and films can be tailored by varying the structure of the underlying solid substrate.

Below, we highlight specific examples and models we used in these studies. All these examples illustrate the extent to which variations in polymer/surface microstructure affect the macroscopic properties of the interface. (Space does not permit detailed discussions of the methodologies, which can be found in cited references.)

Dr. Balazs was born in Budapest, Hungary, in 1953. She received an A.B. degree from Bryn Mawr College in 1975 and a Ph.D. in materials science from the Massachusetts Institute of Technology in 1981. Dr. Balazs is currently the Bicentennial Engineering Alumni Faculty Fellow and Associate Professor in the Materials Science and Engineering Department at the University of Pittsburgh. Her research involves using statistical mechanics and computer simulations to model polymeric systems. Her current research is focused on modeling the properties of polymer blends, the aggregation of associating polymers, and polymer–surface interactions.

Chains at Penetrable Surfaces

Effect of Copolymer Sequence Distribution. We start by considering the behavior of copolymers at penetrable interfaces, such as the boundary between two immiscible liquids or two incompatible homopolymers. Recently Marques and Joanny[4] and Garel et al.[5] studied the behavior of a random copolymer at a liquid–liquid interface. A random copolymer contains two or more types of monomers randomly arranged along the backbone of the chain. However, the arrangement or sequence distribution of the different monomers can vary widely from random to blocky or purely alternating. (Blocky copolymers contain long sequences of the same monomer within the copolymer chain.) We use both analytic arguments and molecular dynamics simulations to determine how the sequence distribution affects the adsorption and conformation of a single copolymer at the boundary between two immiscible fluids.[6]

As in the previous studies,[4,5] we will assume that the liquid–liquid interface remains fixed in space and is perfectly sharp. The polymer is represented by a non-self-avoiding (Gaussian) chain composed of two different monomers, A and B. The monomer–solvent interaction energies are taken to be symmetric: $-\Delta$ for a monomer in the favorable solvent and $+\Delta$ in the unfavorable one. We neglect interactions between the monomers along the chain.

Let the variables P_A and P_B be the fraction of A and B sites, respectively, in a single polymer chain. Given a site A in the chain, the parameter $P_{A\to B}$ yields the conditional probability that the next site is a B site. We now introduce the parameter f, which characterizes the sequence distribution in the chain. The value of f is defined through the following equation:

$$P_A P_{A\to B} = (P_A P_B)^{1/2} f \qquad (1)$$

where f lies between 0 and 1. For the sake of simplicity,

(1) Hancock, R. I. In *Surfactants*; Tadros, Th., F., Ed.; Academic Press: London, 1984; pp 287–321.
(2) Napper, D. H. *Polymeric Stabilization of Colloidal Dispersions*; Academic Press: London, 1983.
(3) Ward, R. S. *IEEE Eng. Med. Biol. Mag.* **1989**, *6*, 22–25.
(4) Marques, C. M.; Joanny, J. F. *Macromolecules* **1990**, *23*, 268–276.
(5) Garel, T.; Huse, D. A.; Leibler, S.; Orland, H. *Europhys. Lett.* **1989**, *8*, 9–13.
(6) Yeung, C.; Balazs, A. C.; Jasnow, D. *Macromolecules* **1992**, *25*, 1357–1360.

0001-4842/93/0126-0063$04.00/0

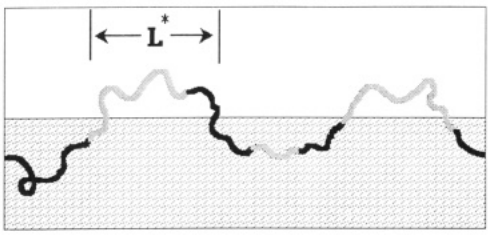

Figure 1. Schematic drawing of AB copolymer at the interface between two immiscible fluids or polymers. The chain forms loops of length L^* on either side of the interface.

we will study the symmetric case where $P_A = P_B = 0.5$. For these values, $f = 1$ corresponds to an alternating chain, $f = {}^1/_2$ represents a purely random chain, and $f \rightarrow 0$ corresponds to a blocky copolymer. We note that $1/f$ corresponds to the average block length. Garel et al.[5] showed that as the chain length approaches infinity, a random copolymer ($f = {}^1/_2$) will always be localized at the interface. By altering the value of f, we can determine the behavior of other symmetric copolymers at this penetrable surface.

To estimate the free energy of the chain at the interface, we assume that the chain weaves back and forth across the boundary, forming loops L monomers in length, on either side of the interface (see Figure 1). Consider the energetics of such a loop. The energy will be minimized by having all monomers of one type on one side of the interface and all monomers of the other type on the opposite side. Therefore, loops of average block length $1/f$ are favored energetically. On the other hand, a small loop will have a large entropy cost. Balancing these effects and including the fact that the sequence of monomers along the chain is correlated, we can write down an effective free energy as a function of the average loop length L and parameter f. (We actually need to consider two adjacent loops to include the effect of the sequence distribution.) We then minimize the resulting free energy to find the optimal loop length L^*. In Figure 2a, we have plotted L^* vs $f/(1 - f)$ on a log–log scale, for several values of Δ/T, where T is temperature.

A surprising result is that, for fixed Δ/T, L^* has a minimum at a finite value of f. Hence, this analysis indicates that there is a specific sequence distribution for which the chain is maximally localized at the interface.

An additional interesting feature is the fact that as $f \rightarrow 0$, L^* does not depend on the amplitude of Δ/T. In this limit, the chain contains long blocks of A and B. For $\Delta > 0$ and sufficiently small f, segregation of entire blocks minimizes the free energy. In other words, loops on average size $1/f$ (the structural correlation length) will form. Since we have assumed a Gaussian chain, the polymer will be localized at the interface with an average width, $W \sim L^{1/2} \sim f^{-1/2}$. We refer to this regime as the strong interaction limit; here, energetic effects dominate the behavior of the chains at the interface.

In the opposite limit, to which we refer as the weak interaction limit, the balance between entropic and energetic contributions is important. In this limit, we find that L^* behaves as[6]

$$L^* \sim \left(\frac{T}{\Delta}\right)^2 \frac{f}{1-f} \qquad (2)$$

From eq 2, we see that L^* increases as $f/(1 - f)$ with

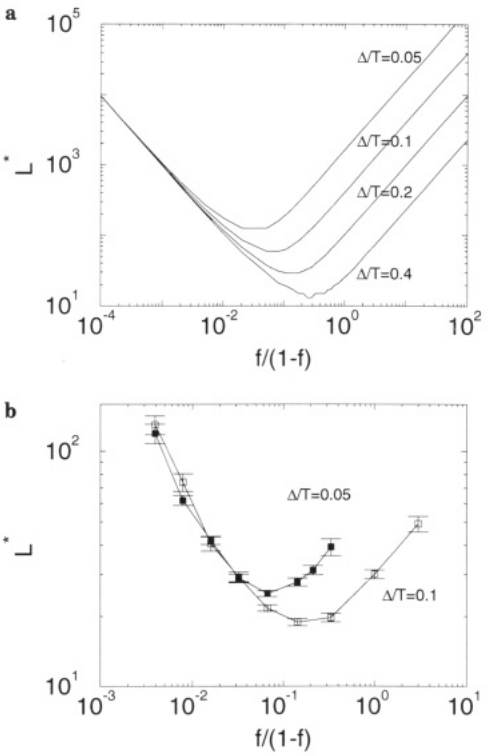

Figure 2. (a) L^* vs $f/(1 - f)$ on a log–log scale. As $f \rightarrow 0$, $L^* \rightarrow 1/f$, while in the weak interaction limit, $L^* \sim f/(1 - f)$ as $f \rightarrow 1$. (b) L^* vs $f/(1 - f)$ on a log–log scale obtained from molecular dynamics simulations.

increasing f, giving the behavior to the right of the minima in Figure 2a. Furthermore, L^* decreases with an increase in Δ. In the weak interaction limit, the Gaussian chain is localized with width $W \sim (L^*)^{1/2} \sim (T/\Delta)(f/(1 - f))^{1/2}$. (Note that the above equation displays a singularity at $f = 1$, which indicates that other techniques are needed to analyze this limiting behavior. The behavior of W for a purely alternating copolymer is discussed below.)

To test these predictions, we performed a series of molecular dynamics simulations. The details of the calculation are given in ref 6; here we just present the results of that study in order to demonstrate the agreement between the analytical model and the simulation. Specifically, Figure 2b shows the plot of L^* versus $f/(1 - f)$ obtained through the molecular dynamics calculations. As predicted, the curves have a well-defined minimum and are independent of Δ/T for small f(long block lengths).

The results have significant implications for tailoring chains to optimize the desired interfacial properties. First, consider the penetrable interface to represent the boundary between two immiscible low molecular weight fluids. In this case, the sequence distribution which corresponds to the minimum in the curves constitutes an optimal architecture for a copolymer additive. By forming small loops and frequently intersecting the boundary, this architecture will be most efficient at reducing the interfacial tension.

We can also consider this penetrable boundary to represent the interface between two incompatible homopolymers. (In this case, the physical interface may not be as sharp. The width of this interface will depend, in part, on the interaction energy between the two homopolymers. Specifically, the width decreases

as the incompatibility is increased. Thus, the interface will be sufficiently narrow for highly immiscible homopolymers.) Recent studies by Kausch and Tirrell[7] and Kramer et al.[8] indicate that, in order for copolymers to act as adhesives, which effectively "stitch" phase-separated homopolymers together, the copolymers must make long excursions back and forth across the penetrable interface. Our results indicate that chains at both ends of the sequence distribution spectrum, namely, multiblocks with long segments of A's and B's and alternating-like copolymers, will provide this optimal behavior. Thus, our predictions can also be used to design the optimal copolymer additive for improving the internal adhesion and mechanical integrity of immiscible polymer blends.

Alternating Copolymers: Effect of the Monomer–Solvent Interaction Energies. As noted above, for an AB copolymer displaying a strictly alternating pattern (...ABABAB...) along its backbone, we must resort to a different analysis in order to determine the dependence of W (the localization width) on the interaction strength, Δ. Using numerical methods and analytical techniques,[9] we find that, in the "weak interaction" region, $W \sim \Delta^{-2}$. This is a different scaling relationship than that obtained for the other polymer architectures within this regime (see eq 2). These findings indicate the sensitivity of the adlayer to variations in copolymer architecture.

We can also consider the effect of fixing the polymer architecture, but varying the relative affinities between the monomers and the two fluids.[9] Through this study, we can determine what happens when the monomer–solvent interactions are asymmetric. We again consider the alternating copolymer described above; however, we now distinguish Δ_A as the A–solvent interaction energy, while Δ_B represents the B–solvent energy. The interface between the two immiscible fluids is represented by the $Z = 0$ plane. For $\Delta_A, \Delta_B \geq 0$, the A monomers prefer the $Z > 0$ region, while B monomers favor the $Z < 0$ domain. We now consider the case where $\Delta_A \neq \Delta_B$.

Figure 3 shows the density profile for the copolymer at the interface for two different (Δ_A, Δ_B) pairs. For the case where $(\Delta_A, \Delta_B) = (0.7, 0.6)$, the profile is strongly peaked, indicating that the chain is highly localized about the interface. On the other hand, for the (0.69, 0.59) example, the density profile and the chain are more spread out, indicating that the chain is no longer confined at the interface.

From a series of similar calculations, we can generate the phase diagram shown in Figure 4, which indicates, as a function of Δ_A and Δ_B, where the chain is localized (L) at the interface or preferentially "delocalized" in one of the two fluids (D_+ or D_-). In the latter case, the chain drifts away from the interface and is located in one fluid or the other. These results again aid in isolating conditions under which the copolymers will be most effective at modifying the interfacial properties.

(7) Kausch, H. H.; Tirrell, M. *Annu. Rev. Mater. Sci.* **1989**, *19*, 341–377.
(8) Creton, C.; Kramer, E. J.; Hui, C.-Y.; Brown, H. R. *Macromolecules* **1992**, *25*, 3075–3088.
(9) Li, W.; Yeung, C.; Jasnow, D.; Balazs, A. C. *Macromolecules* **1992**, *25*, 3685–3688.

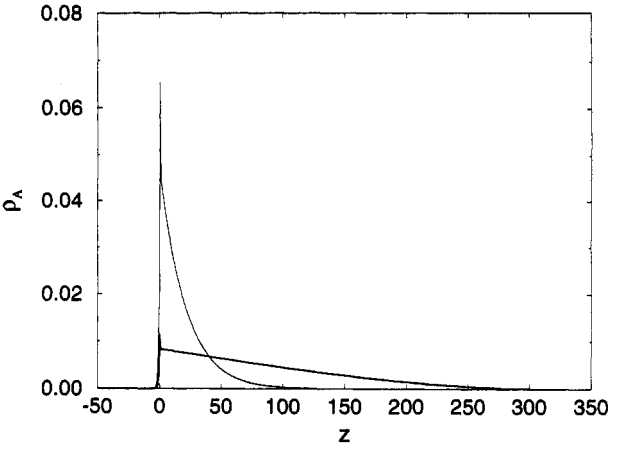

Figure 3. Density profiles at two points $(\Delta_A, \Delta_B) = (0.7, 0.6)$ (the narrower curve) and (0.69, 0.59) (the wider curve). Reprinted with permission from ref 9. Copyright 1992 American Chemical Society.

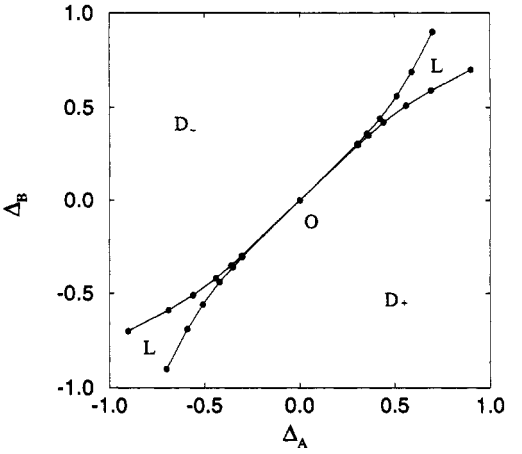

Figure 4. Phase diagram in the $\Delta_A - \Delta_B$ parameter space. D_+ and D_- are phases where the polymer is delocalized in the $Z > 0$ and $Z < 0$ regions, respectively. L is the localized phase. Reprinted with permission from ref 9. Copyright 1992 American Chemical Society.

Chains at Impenetrable Surfaces

Chemically Heterogeneous Surfaces. The performance of polymer films, polymer coatings, and polymer–ceramic and –metal composites depends in large part on the adsorption and adhesion of polymers to the substrate. Substrates are commonly composed of more than one material, either through design or due to the presence of impurities. In previous theories for polymer adsorption, it was assumed that the surface is chemically uniform. To study more realistic surfaces, we introduced a self-consistent-field lattice model for copolymer adsorption onto laterally heterogeneous surfaces.[10] In a self-consistent-field theory, the many-polymer problem is treated as independent polymers in an average potential of the other chains. This potential is calculated in a self-consistent manner. The model allows us to calculate equilibrium adsorption profiles for copolymers on a variety of substrates. Consequently, we can undertake fundamental studies on the behavior of macromolecules at nonhomogeneous, solid interfaces.

In our study, we consider the substrate to be composed of strips of two different materials, S1 and S2 (see Figure

(10) Huang, K.; Balazs, A. C. *Phys. Rev. Lett.* **1991**, *66*, 620–623.

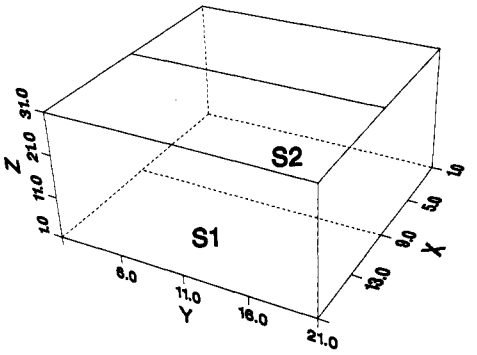

Figure 5. The three-dimensional lattice used in the calculation. Periodic boundary conditions are applied along the Y direction of the box.

5). (Experimentally, analogous surfaces can be fabricated through microlithography.[11] The solution above the surface contains AB diblock copolymers. In our calculation, the diblock is composed of 25 contiguous A monomers linked to 25 B's. The parameter χ_{ij} describes the interaction energies between the i and j species; positive values of the parameter indicate a repulsive interaction, while negative values represent attractive interactions.[12] Here, we set $\chi_{AB} = 0.5$; the interaction energy between A and the solvent is equal to 0.5, while the interaction between B and the solvent is 0.0. Thus, the solution is a θ solvent for the A moiety, but an athermal solvent for the B block. The solvent–surface interaction energy is set equal to 0.0 for both S1 and S2.

While the chains are free to diffuse in the solution, the A block has an affinity for S1, and the B block is attracted to S2. Can we tailor the A–S1 and B–S2 enthalpies such that the chains adsorb from solution and the polymer–surface interactions induce a phase segregation at the interface, namely, that the A blocks are localized on S1 and the B blocks are segregated to S2? The answer is revealed in Figure 6. The figure shows the polymer density in the layer directly above the surface, the $Z = 2$ layer, versus distance along the X direction. The region on the left, $X = 1$–8, represents the S1 domain, and $X = 9$–16 represents the S2 region. The solid curves describe the volume fraction of A molecules in the $Z = 2$ layer, while the dashed curves represent the volume fraction of B molecules in this layer. The curves describe the experiment in which $\chi_{A\text{-}S1}$ and $\chi_{B\text{-}S2}$ are both set equal to −10.0, while $\chi_{A\text{-}S2} = \chi_{B\text{-}S1} = 0$. As can be seen, due to the strong affinities for the respective surfaces, the A segments are segregated to the S1 domain and the B blocks are localized on the S2 region. (Since the B segments are not repelled from the solvent, there is slightly less of the B blocks adsorbed onto the surface.)

In a second experiment, we maintain $\chi_{A\text{-}S1}$ and $\chi_{B\text{-}S2}$ at −10.0; however, we now introduce a finite attraction between A and S2, as well as between B and S1, by setting $\chi_{A\text{-}S2} = \chi_{B\text{-}S1} = -5.0$. Despite this change, the resulting polymer density profiles are essentially identical to the ones in Figure 6. Even though the A's have

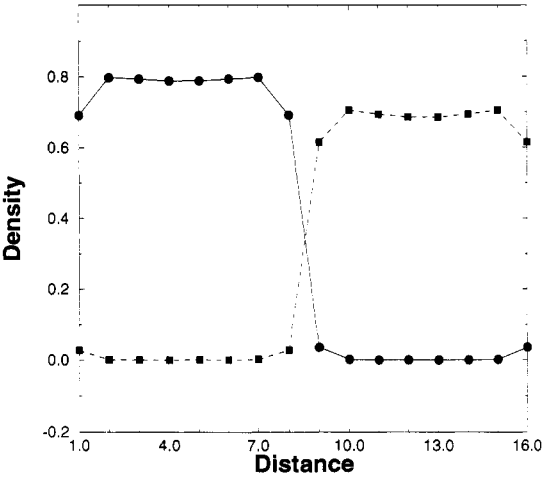

Figure 6. The solid line (with filled circles) represents the volume fraction of adsorbed A in $Z = 2$, while the dashed line (with dark squares) depicts the volume fraction of adsorbed B in this layer. For these curves, $\chi_{A\text{-}S1} = \chi_{B\text{-}S2} = -10$ and $\chi_{A\text{-}S2} = \chi_{B\text{-}S1} = 0$. The volume fraction of copolymer in the bulk solution, ϕ_b, is equal to 10^{-4}.

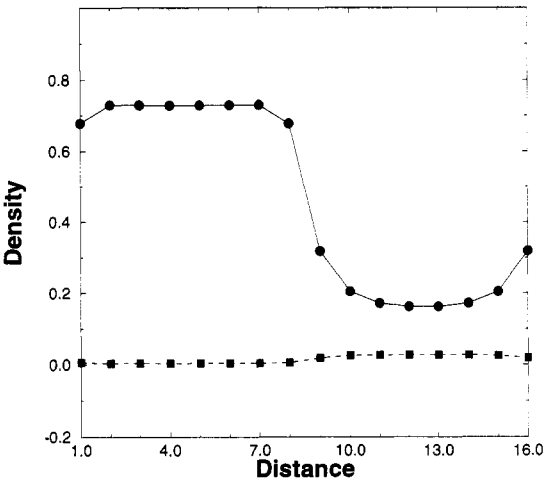

Figure 7. The solid line (with filled circles) represents the volume fraction of adsorbed A in $Z = 2$, while the dashed line (with dark squares) depicts the volume fraction of B in this layer. For these curves, $\chi_{A\text{-}S1} = -10$, $\chi_{A\text{-}S2} = -5$, and $\chi_{B\text{-}S1} = \chi_{B\text{-}S2} = 0$. (The increase in A density at $X = 16$ is due to the periodic boundary conditions that are imposed along Y.) Again, $\phi_b = 10^{-4}$.

an affinity for S2, these blocks are excluded from this region by the more strongly attracted B's. In the same manner, the B's are excluded from S1. In effect, the more energetically favored interactions dominate and the phase segregation is again observed.

From the above experiment, we could hypothesize that if we effectively removed the B–surface interactions, the A sites would "spill over" onto the S2 domain. This phenomenon is indeed observed in Figure 7, which shows the polymer density profile that results from setting $\chi_{B\text{-}S2} = \chi_{B\text{-}S1} = 0$, while keeping the A–surface interactions the same as above. Now, there is a significant fraction of A sites on S2; however, since $\chi_{A\text{-}S1} > \chi_{A\text{-}S2}$, there is a higher volume fraction on the S1 domain.

In the final experiment, we again set $\chi_{A\text{-}S1} = \chi_{B\text{-}S2} = -10.0$ and $\chi_{A\text{-}S2} = \chi_{B\text{-}S1} = 0.0$. However, we change the polymer architecture from diblock to an alternating multiblock, which contains a block of five A's next to a block of five B's along the length of the chain. Despite

(11) Laibinis, P. E.; Hickman, J. J.; Wrighton, M. S.; Whitesides, G. M. *Science* **1989**, *245*, 845–848.

(12) The χ's for this lattice model are higher than experimental Flory–Huggins χ parameters since they also include a multiplicative factor that accounts for the number of nearest neighbors in the lattice. For a further discussion of this point, see: Evers, O. A.; Scheutjens, J. M. H. M.; Fleer, G. J. *J. Chem. Soc., Faraday Trans.* **1990**, *86*, 1333–1340.

the strong polymer–surface selectivities, the polymer segregation noted in Figure 6 is destroyed. Now A sites are found on S2 and B sites are located on S1. Here, the length of the A block is sufficiently shorter than the S1 domain; thus, when the A sites stick, neighboring B's are also dragged down onto the S1 region. (When B's bind to S2, neighboring A's are also dragged down onto S2.)

The above result indicates that the equilibrium properties of chains adsorbed onto laterally heterogeneous surfaces depend not only on the relevant interaction energies but also on the polymer architecture. For sufficiently attractive energies, the diblocks can undergo a phase segregation on the surface. However, strong segregation depends on matching the length of the block to the length scale of the surface heterogeneity. These predictions are useful in designing interfaces that contain well-defined, ordered domains of different macromolecules. Such materials can be tailored to display unique electrical and optical properties, which can be used in a variety of technological applications.

Lateral Instabilities in Grafted Homopolymers. The previous findings revealed how to fabricate patterned films and coatings by exploiting chemical variations in the copolymer and the underlying substrate. We also observed a way to produce lateral variations in homopolymers on homogeneous surfaces. The architectural feature that is essential to producing this effect is that the homopolymers are end-grafted: one end of each chain is fixed on a solid surface. In a good solvent the polymer layer is laterally uniform or homogeneous. However, placing the grafted layer in a poor solvent drives increases in the local monomer concentration. If the polymer ends were free to move on the grafting surface, this may result in global phase separation: there would be macroscopic regions of the grafting surface in which the polymer concentration is high and other regions in which it is low. Since the chains we consider are grafted, global phase separation is not possible but the increase in the local polymer concentration may occur by uniform compression of the layer normal to the grafting plane and/or by local clumping of polymer chains in the lateral direction.[13]

To determine the effect of a poor solvent, we first use a one-dimensional self-consistent field method, which assumes that the polymer layer is homogeneous parallel to the grafting plane. We then apply the random phase approximation (RPA) to treat the effect of perturbations on the layer. (The latter calculation is also done self-consistently.) Using this method, we determine whether concentration fluctuations in the homogeneous layer will relax, so that the layer remains stable, or grow in size, so that the layer becomes unstable. In the latter case, the concentration fluctuations destroy the lateral homogeneity of the layer, and consequently, some pattern or structure formation will occur. We find that, as a function of chain length, monomer size, grafting density, and solvent quality, there are indeed regions of this parameter space in which the homogeneous layer is unstable; hence, we determine the phase boundary separating the stable from unstable regions.[14] These parameters also characterize the morphology of the structures in the unstable region.

(13) Lai, P.-Y.; Binder, K. *J. Chem. Phys.* **1992**, *97*, 586–595.
(14) Yeung, C.; Balazs, A. C.; Jasnow, D. *Macromolecules*, submitted.

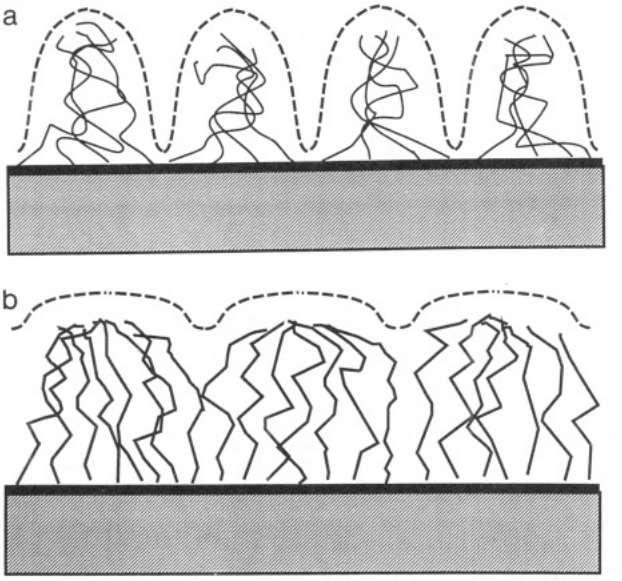

Figure 8. (a) A schematic showing the types of structures expected for short chains. (b) A schematic showing the types of structures expected for longer chains.

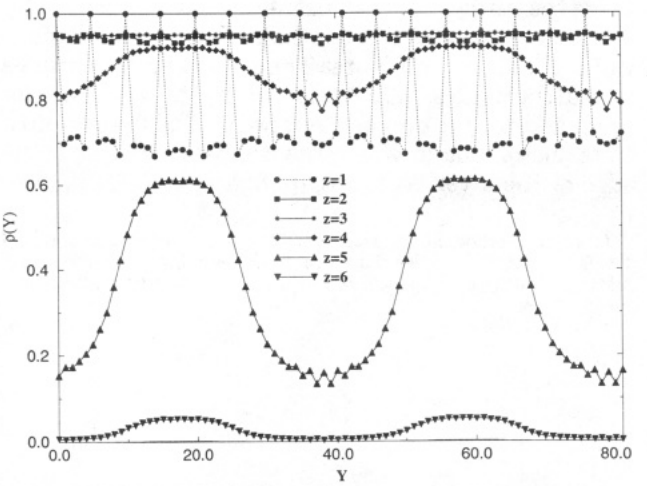

Figure 9. Polymer density profiles along the Y-axis (in the plane of the grafting surface) for various values of Z (the Z-axis lies perpendicular to the grafting plane). The $Z = 0$ plane represents the substrate. The density profiles in the $Z = 1$ and $Z = 2$ layers reflect the grafting pattern. The monomer–solvent interaction energy is equal to 2.35.

In characterizing the unstable region, we find that the instability occurs at finite wavelength, indicating that the chains clump together to form a "dimpled" surface. For shorter chains, the depths of the dimples approximately equal the layer height, and the mean distance between dimples is proportional to the radius of gyration of the chain in a θ-solvent (shown schematically in Figure 8a). As the chain length is increased, the instability is restricted to a region near the edge of the grafted layer. A dimpled structure is still formed, but the depth of the dimples is now given by the bulk correlation length, and the mean distance between the dimples is larger than the radius of gyration (shown schematically in Figure 8b). We note that this method, numerical self-consistent field plus numerical RPA, is very general and can be applied to a wide class of systems. Previous use of the RPA approximation has been limited to the few cases where an analytic solution to the mean field problem can be obtained.

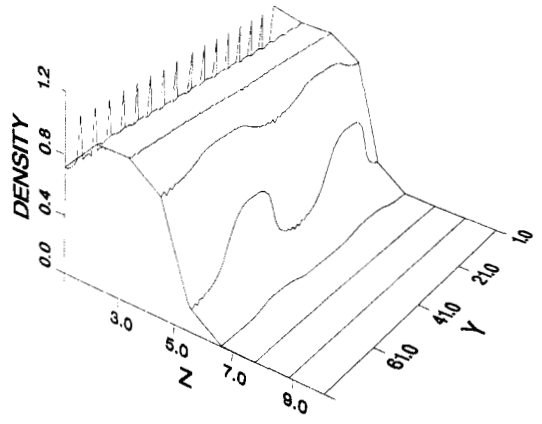

Figure 10. A three-dimensional plot of the data in Figure 9. As noted above, the spikes in the $Z = 1$ and $Z = 2$ profiles reflect the grafting pattern.

To test and extend the above predictions, we went beyond the linear analysis of the random phase approximation and developed a two-dimensional numerical mean field model for grafted chains.[15] In this model, the chains are grafted at approximately periodic points along the surface. With this method, we can explicitly calculate density profiles for the grafted homopolymers, which are shown in Figures 9 and 10. As can clearly be seen in the figures, the density profiles show the dimples predicted by our previous analysis. The figures illustrate the regime in which the dimples occur near the edge of the layer, as in Figure 8b.

(15) The method is an extension of the one-dimensional model developed by S. J. Hirz. See: Hirz, S. J. Modeling of Interactions Between Adsorbed Block Copolymers. Masters Thesis, University of Minnesota, 1986.

Concluding Remarks

The results from these studies help establish design criteria for the control of polymeric interfaces. In particular, we discuss the optimal macromolecular architecture for penetrable interfaces. This is relevant to the design of stable oil–water emulsions and the fabrication of polymer blends with superior mechanical properties. Additionally, we discuss the behavior of polymers at impenetrable interfaces and indicate how to create adsorbed polymer films with well-defined heterogeneities or patterns. These guidelines will facilitate the development of coatings for optical or electronic devices. Our studies on grafted layers are important for preparing multilayer coatings, where the first or primer layer governs the degree of adhesion between the substrate and a subsequent polymer coating. From these various applications, ranging from oil–water emulsions in petroleum processing to surface modification and adhesion, it is clear that the interfacial properties of copolymers play a critical role in several important chemical manufacturing processes.

This work was done in collaboration with several people: postdoctoral associates Chuck Yeung and Weixiong Li, graduate student Kanglin Huang, and Professor David Jasnow (Physics Department). As always, I thank Dr. Christopher Lantman for his editorial help. I gratefully acknowledge financial support from the Department of Energy through Grant DE-FG02-90ER45438, the National Science Foundation through Grant DMR-9107102, the Office of Naval Research through Grant N00014-91-J-1363, and The Dow Chemical Company.